Fire Safety Journal 82 (2016) 37–48

Contents lists available at ScienceDirect

Fire Safety Journal

journal homepage: www.elsevier.com/locate/firesaf

Elevated temperature behaviour and fire resistance of cast iron columns

C. Maraveas *, Y.C. Wang, T. Swailes

School of Mechanical, Aerospace and Civil Engineering, University of Manchester, UK

ARTICLE INFO

Article history:
Received 9 July 2015
Received in revised form
7 February 2016
Accepted 26 March 2016

Keywords:
Columns
Cast iron
Fire resistance
Imperfections
Restraints
Load factor

ABSTRACT

Cast iron columns were used in many 19th century structures. Many such structures are still in use today and it is important that they fulfill the current requirements on fire resistance. This paper presents the results of a comprehensive study of the behavior and fire resistance of cast iron columns based on extensive numerical simulations using ABAQUS. The ABAQUS simulation model was validated against six fire tests performed in the USA in 1917. The validated model was then used to investigate the effects of several parameters (column slenderness, load factor, load eccentricity, imperfections of column and cross section, axial restraint) on the behaviour of cast iron columns in fire. The parametric study results indicate that the fire resistance is governed by the applied load and these columns are sensitive to load eccentricity. Based on a comparison between the numerical simulation results and predictions of the EN 1993-1-2 method which is for modern steel structures, it has been found that the EN 1993-1-2 method can give safe and reasonably accurate estimate of the strength and fire resistance of cast iron columns.

1. Introduction

Cast iron possesses high strength in compression and was ideal for use as columns [1]. Cast iron columns were used for more than 100 years [2] before being replaced by steel as supports to timber, cast iron, wrought iron and steel girders in numerous 19th century historical structures. The ambient temperature behaviour of cast iron columns has been investigated by several researchers [3–7]. However, the behavior in fire of cast iron columns has been based on general observations of fire accident investigations [8–17] and standard fire resistance tests [18,19,20]. However, many such historical reports are not available today and the available fire accident investigation and standard fire test reports do not give detailed data and explanations to allow development of thorough understanding of their behavior in fire. Furthermore, there was no reported follow-up detailed research after these investigations and fire tests.

Many such structures are still in use today and there is a need to quantify their fire resistance. Yet a reliable method for assessing the fire resistance of cast iron columns is lacking. Without carrying out detailed research studies, some researchers [21,22] have proposed to use the Eurocode method for steel structures [23] to assess the fire resistance of cast iron columns. However, there are significant differences between cast iron columns and steel columns, because (1) their mechanical properties are different; and (2) cast iron columns have varying cross-sections due to 19th century casting methods. Therefore, extrapolating the steel column design method to cast iron columns may not be appropriate and further systematic investigations are clearly necessary.

The objective of this paper is to carry out detailed numerical investigations of cast iron columns and to use the simulation results to develop an analytical method that may be adopted in assessment of fire resistance of cast iron columns. Validation of the numerical simulation model, developed using the general finite element software ABAQUS, is established by comparison against available fire test reports. The mechanical properties are based on the model developed by the authors following a comprehensive review of the available test data [24] as well as the authors' new test data [25].

The numerical model considers the effects of imperfections in the cast iron cross-sections and initial imperfections. The parametric study, using the validated numerical simulation model, examines the effects of changing load ratio, load eccentricity, axial restraint, cross-section and member imperfections and column slenderness on cast iron column behavior and fire resistance. The results of this parametric study are then used to assess applicability of EN 1993-1-2 [23], which is for modern steel structures, to historic cast iron columns.

* Corresponding author.
E-mail address: c.maraveas@maraveas.gr (C. Maraveas).

http://dx.doi.org/10.1016/j.firesaf.2016.03.004
0379-7112/

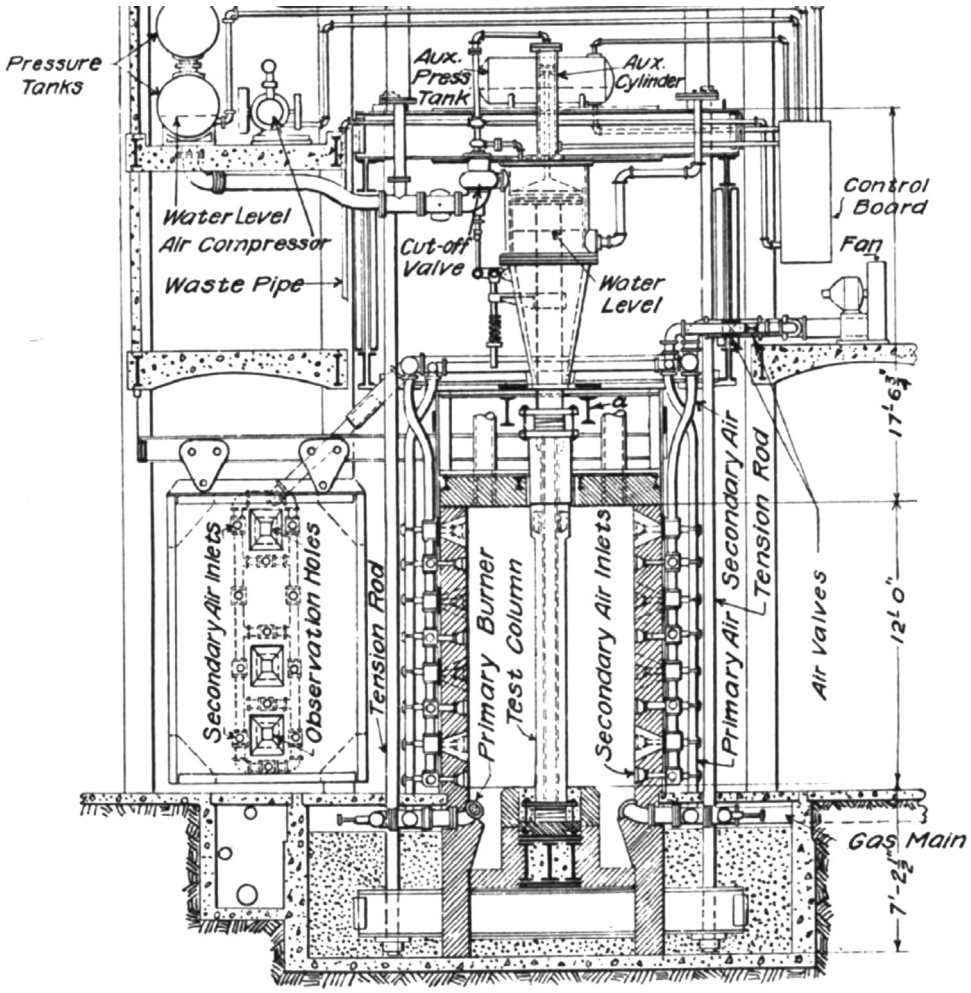

Fig. 1. Elevation of fire testing facility [19].

2. Fire tests

Between 1917 and 1919, 106 steel, cast iron, reinforced concrete and timber column fire tests were conducted at the Underwriters' Laboratories in Chicago, Illinois, USA [19]. Amongst these fire tests, some had unprotected cast iron columns and some had protected cast iron columns. Three of the unprotected cast iron columns, No. 9, 10 and No 10a, and four of the protected cast iron columns (No. 27, 47, 62 and 63), were fully instrumented and the test report has provided detailed information on the temperature and deflection histories of the columns. These fire tests will be used for validation of the simulation model of this paper.

The fire tests [19] were performed in a gas furnace as illustrated in Fig. 1. Fig. 2a shows the column geometry for columns No. 9 and 10. The columns had a nominal external diameter of 7 in (177.8 mm) and internal diameter of 5½ in (139.7 mm). However, there were imperfections in the cross-sections and the wall thickness varied by as large as 1/4 in (6.35 mm). The cross section imperfection has been assumed as uniform along the length of the columns as further information are not provided in [29]. Fig. 3a shows the actual recorded column cross-section dimensions. The vertical imperfection (at the middle of the column) was 1/8 in (3.18 mm). The length of the tested columns was 4.78 m. Table 1 summarises the cross-sectional and length imperfections of the columns.

All test columns had insulated heads as shown in Fig. 2b, so the fire exposed length of the columns was 3.76 m.

Both column ends in fire test No. 9 were assumed to be rotationally fixed because the bolted end plates were considered to offer a substantial amount of rotational restraint. Because the fixing bolts and end plates were cast in and, therefore insulated by, concrete as indicated in Fig. 1, the rotationally fixed condition was considered to have been maintained during the fire test. The top end in fire tests Nos. 10 and 10a was rotationally fixed but the bottom was considered to be simply supported (Fig. 2d). The assumed boundary conditions to other columns, based on the test report, are listed in Table 1.

The protected columns (Nos. 27, 47, 62 and 63) had the same nominal dimensions and test arrangement as the unprotected column No. 9. The fire protection provisions for the columns were:

- No. 27 (Fig. 4a): 1½ in (38.1 mm) thick Portland cement plaster in ribbed expanded metal lath with 1/2 in (12.7 mm) of broken air space (Fig. 3b);
- No. 47 (Fig. 4b): 2 in (50.8 mm) Portland cement, Long Island sand and Hard coal cinders (mixture 1:3:5) (Fig. 3c);
- Nos. 62 and 63 (Fig. 4c): porous semi-fired clay (52.3 mm) on 3/4 in (19 mm) of mortar (Fig. 3d).

The applied load was 95,500 lb (approximately 425 kN) for all columns except 10a on which the applied load was 98,500 lb (approximately 438 kN). These loads gave an average stress of 45 MPa, which was the maximum permitted stress according to the then US specifications (10,000–60*l/r, where l/r is slenderness ratio). This stress is similar to the maximum permitted value by the 1909 London Act [26].

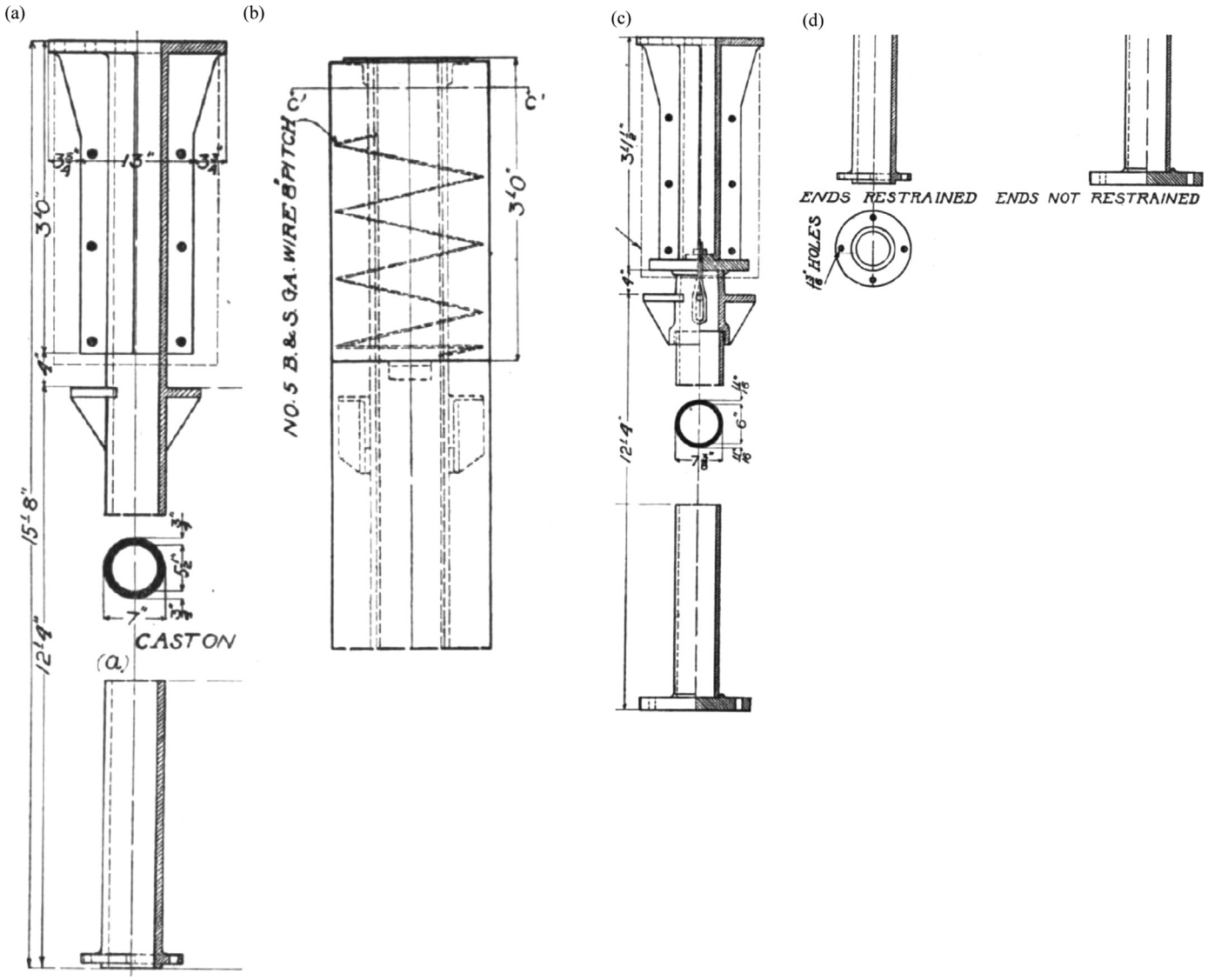

Fig. 2. (a) Geometry of tested cast iron columns No. 9 and 10 and (b) Details of the column's head fire protection, (c) Geometry of tested cast iron column No. 10a and (d) base plate depending the use of bolts or not [19].

Table 1 summarizes the fire test results. The maximum temperatures of all the columns at failure were between 694 °C and 760 °C. The column failure was initiated by compressive failure of the thin part of the cross section, leading to failure of the thick part of the cross section and the entire column. All columns experienced large displacements at failure. Fig. 4 shows the deformed shape of the columns after the fire tests.

3. Simulation model

The general finite element software ABAQUS was used for both thermal analysis to calculate the column temperature distributions and for mechanical analysis of the columns at elevated temperatures. 3D thermal analysis was carried out so that the column temperature data could be directed transferred to the structural analysis model. Eight-node hexahedral solid elements were used for both heat transfer analysis and structural mechanical analysis (C3D8i). Fig. 5 shows an example of the finite element mesh. The cross-section shape was assumed to be uniform along the column height based on the assumption that the casting mould would be the same throughout the column length.

3.1. Mechanical and thermal properties of insulations and cast iron

For all columns except Nof 10a, the ambient temperature modulus of elasticity was calculated from the axial load-displacement relationship, giving a value of 103.95 GPa. The fire test report [19] gives a tensile strength of 160.165 MPa (23,230 lb/in.^{2}). The failure tensile strain at ambient temperature was 0.5%, similar to that in [25]. As the 0.2% proof stress was not given in the report, it was assumed to be 60% of the tensile strength. Table 2 lists the key ambient temperature mechanical properties for the different columns.

The reduction of mechanical properties (Young's modulus, yield stress, ultimate stress) of cast iron were assumed to be similar to those for steel in EN 1993-1-2 [23], based on the authors' comprehensive literature review [24,27] and new test data [25]. The stress strain temperature relationships of cast iron were according to the model proposed by the authors [25]. Fig. 6(a and b) shows the resulting stress strain temperature relationships for both tension and compression of cast iron. It should be pointed out that although the proposed stress–strain relationships (trilinear for tension and bilinear for compression) are not curved, they were adopted for simplicity. Nevertheless, they reflect the

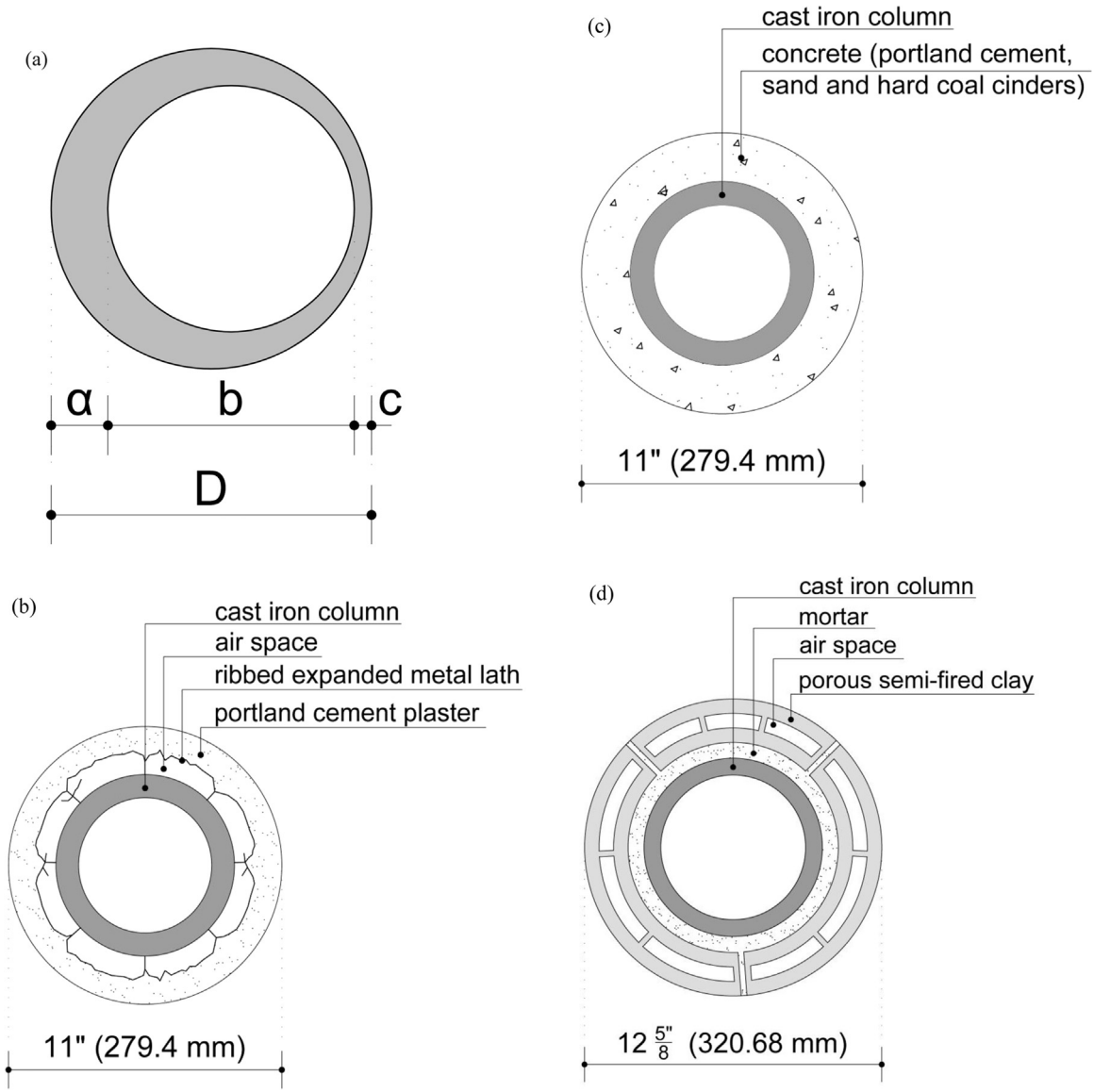

Fig. 3. (a) Geometry of cross section and reference dimensions and insulations for column (b) No. 27, (c) No. 47 and (d) No. 62 and 63 [19].

principal features of cast-iron behavior: largely linear elastic initially, followed by reduced stiffness.

The insulation was assumed not to have any mechanical resistance.

The thermal properties of cast iron were assumed to be the same as those in EN 1993-1-2 [23] for steel. For the different protected columns, the different insulations were assumed to have the following thermal properties, based on the results of

Table 1
Summary of cast iron column fire test specimens and results [19].

Fire test no.	Cross section dimensions (a/b/c/D) (mm)	Load (kN)	Protection	Rotational restraint (top/bottom)	Failure time (min)	Surface temperature at failure (°C)
9	25.4/139.7/12.7/177.8	425	No	Fixed/fixed	34.25	694
10	25.4/139.7/12.7/177.8	425	No	Fixed/fixed	34.5	745
10a	23.39/153.24/10.7/187.33	438	No	Fixed/fixed	34.25	718
27	25.4/139.7/12.7/177.8	425	Portland cement plaster (38.1 mm) in ribbed expanded metal lath with broken air space (12.7 mm)	Fixed/fixed	178	735
47	25.4/139.7/12.7/177.8	425	Portland cement, Long Island sand, Hard coal cinders (1:3:5) (50.8 mm)	Fixed/fixed	168.75	710
62	25.4/139.7/12.7/177.8	425	Porous semi-fired clay (52.3 mm) on mortar (19 mm)	Fixed/fixed	251.5	760
63	25.4/139.7/12.7/177.8	425		Fixed/fixed	177.5	730

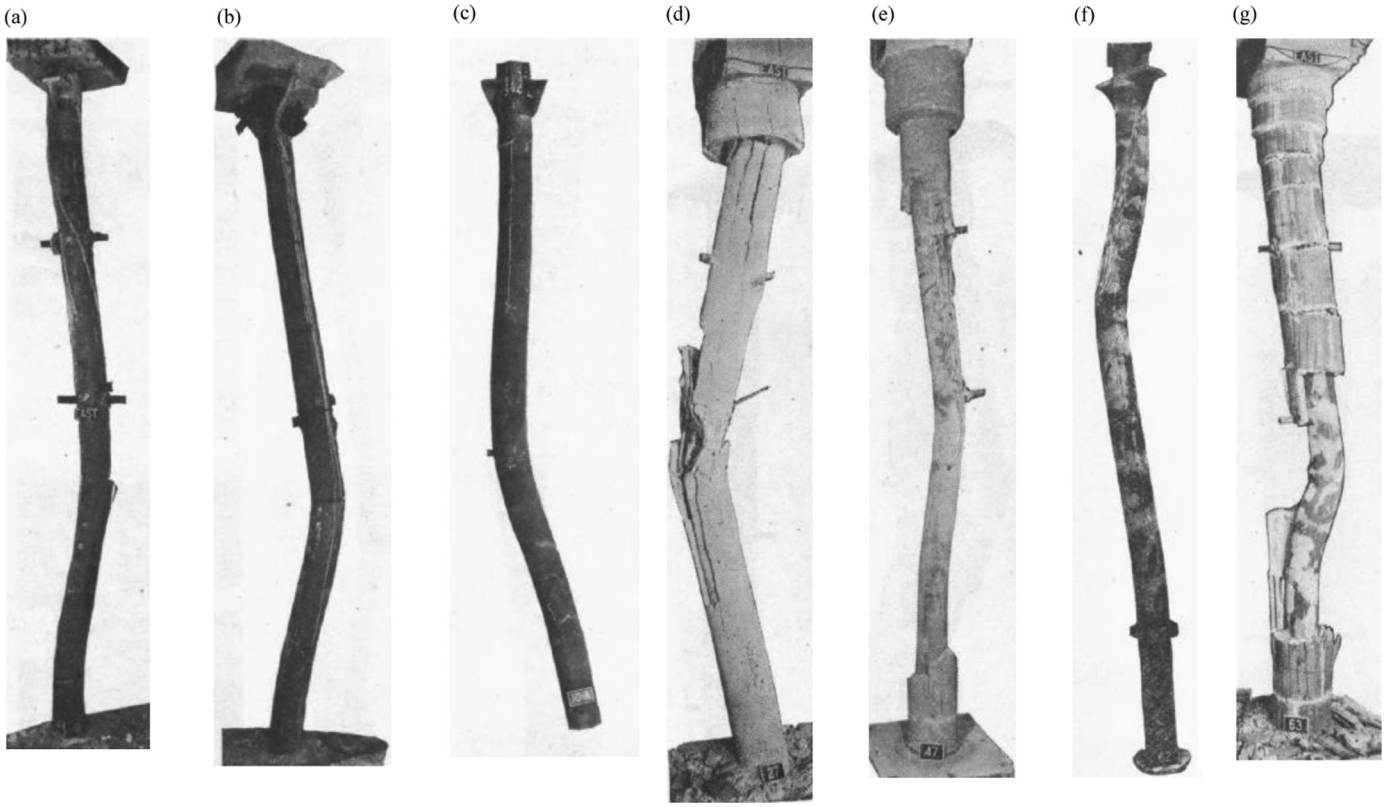

Fig. 4. Deformed columns after fire test (a) No. 9, (b) No. 10, (c) No. 10a, (d) No. 27, (e) No. 47, (f) No. 62 (stripped) and (g) No. 63 [19].

sensitivity study of the authors [27]:

i. Portland cement plaster in ribbed expanded metal lath with broken air space (No 27): use the thermal properties of concrete as in EN 1992-1-2 [28] with the air gap modeled using void radiation emissivity 0.7.
ii. Concrete: Portland cement, Long Island sand, Hard coal cinders (No. 47): use the thermal properties of concrete as in EN 1992-1-2 [28].
iii. Porous semi-fired clay on mortar (Nos. 62 and 63): use the upper bound specific heat and lower bound thermal conductivity for heavyweight masonry units [27]. Model the air gap as cavity radiation with emissivity 0.7.

It was assumed that the insulation and cast iron were in perfect contact.

3.2. Thermal analysis results

The convective heat transfer coefficient was taken as 25 W/m^2 K and the resultant emissivity was taken as 0.7, based on EN 1991-1-2 [29].

Fig. 7 compares the test and simulation temperature results at different locations of the column cross-section for the unprotected columns. Due to non-uniform thickness of the cross-section, the temperatures at different locations of the cross-section were clearly different, with temperatures in the thicker part of the cross-section being lower than those in the thinner part. The numerical simulation results closely follow this trend and give very similar values as the test results for the different measurement locations although slightly higher. It should be pointed out that there was no temperature record for the thinner part of the cross-section (nodes 3 and 4) in [19] and they were expected to follow the maximum temperatures. Similarly, the simulation temperatures for nodes 1 and 2 (where the cross-section thickness is the maximum) should be compared with the measured minimum temperatures.

Fig. 8 compares the measured and simulation temperatures in the cross-section of the protected columns ((a) No. 27, (b) No. 47 and (c) No. 62). Because the assumed thermal properties of the insulation materials may be different from the actual ones (the data were not available), there are some difference between the simulation and measured temperature results. Nevertheless, the measured and simulated cast iron temperatures are quite close, particularly after the first hour of the fire test with the difference in temperature being less than 50 °C.

3.3. Structural analysis

Figs. 9, 10 and 11 compare the fire test and numerical simulation results for unprotected columns Nos. 9 and 10 and protected columns Nos. 27, 42 and 62, with Figs. 10 and 11 showing the axial deformation – time relationships and Fig. 11 comparing the deformed shapes, being the only detailed experimental results available in the historical test report. Both figures indicate good agreement between the test and simulation results. The recorded deformed shapes of the columns clearly support the assumed boundary condition that all degrees of freedom were fixed except for the longitudinal direction at the column top and that all the degrees of freedom were fixed at the column bottom (Euler case 4). The relative displacement refers to the difference of displacements at the top and bottom of the fire exposed segment of the column divided by the distance between them. The simulation fire resistance time of 28 minutes compares very favorably with the fire test results of 27 minutes for column No. 9 and 31 min for column No. 10 (Fig. 9).

Table 3 compares the key values between the numerical simulation results with the fire test results. The close agreement

Fig. 5. (a) Finite element mesh of an unprotected cast iron column (No. 9) (34040 elements); (b) finite element mesh for the cross-section.

Table 2
Ambient temperature mechanical properties for tested columns.

Column no.	Young's modulus (GPa)	0.2% Proof stress in tension (MPa)	Tensile strength (MPa)
9, 10, 27, 47, 62	103.95	96.1	160.16
10a	73.72	72.81	121.35

demonstrates validity of the numerical simulation model.

Note Table 3 does not contain results for column No. 63. According to the test report [19], this test column was practically identical to No. 62. But this column failed approximately an hour earlier than column No. 62 and the test report did not provide any explanation.

4. Parametric study

The objective of the parametric study is to examine the effects of changing different design parameters on fire resistance of cast

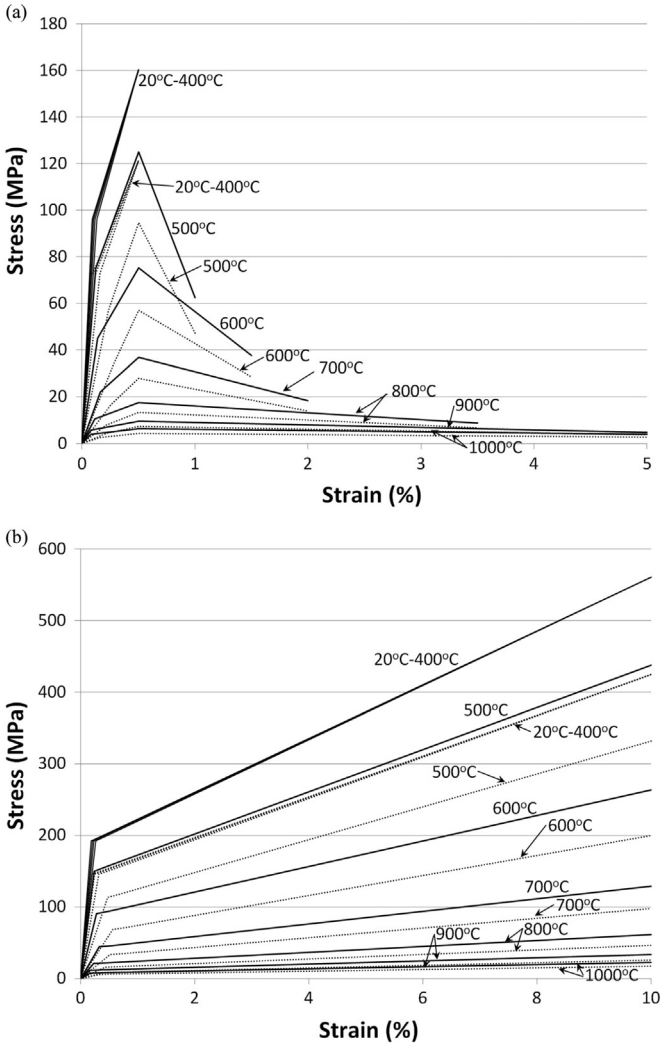

Fig. 6. Stress strain temperature relationships of cast iron for (a) tension, and (b) compression (dotted lines are for column No. 10a).

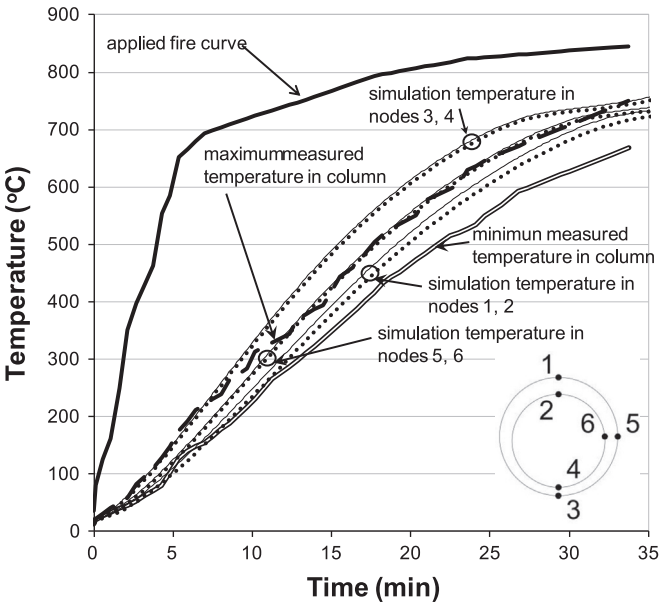

Fig. 7. Comparison of measured [19] and simulation temperature-time curves at different locations for the unprotected columns (Nos. 9 and 10).

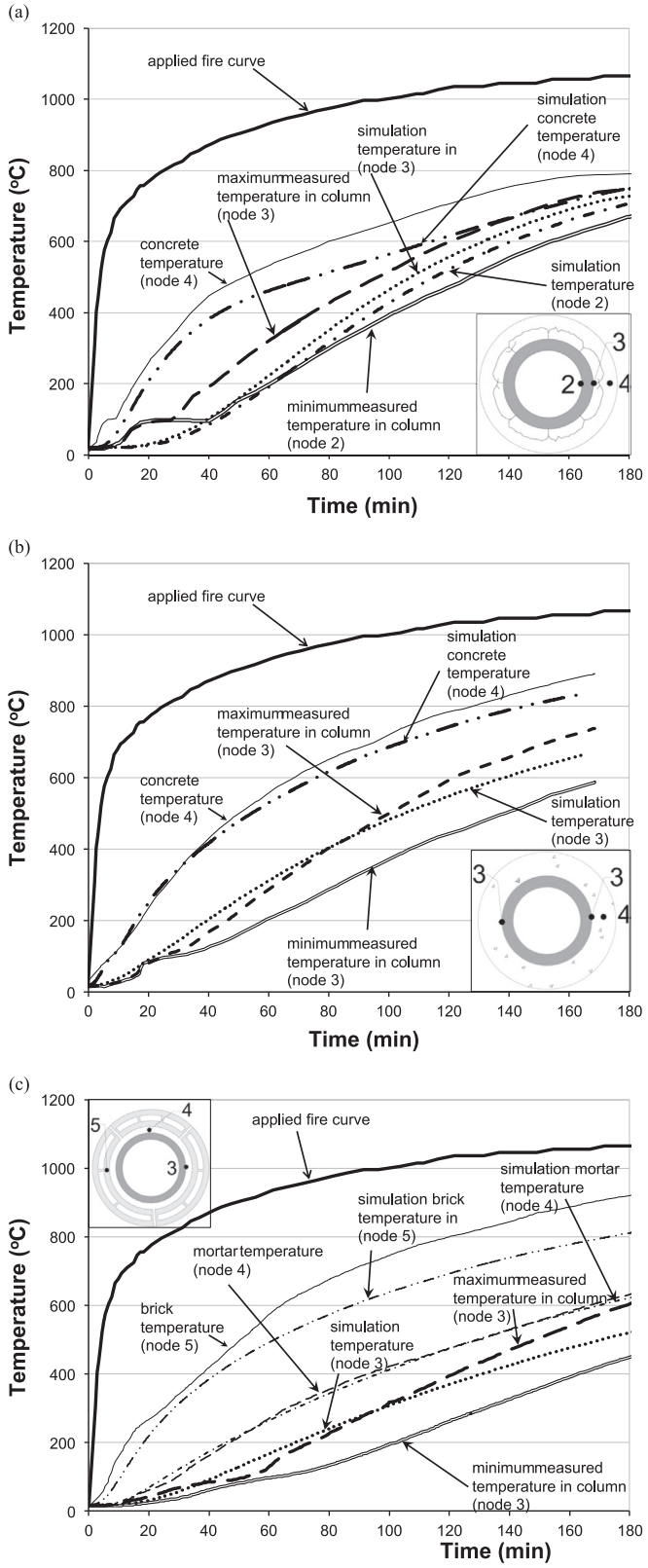

Fig. 8. Comparison of measured [19] and simulation temperature-time curves at different locations of protected columns (a) No. 27, (b) 47 and (c) 62.

iron columns and to use the simulation results to develop an analytical method that may be adopted for design purpose. For this purpose, the following parameters were considered: load factor (ratio of applied load under fire to design resistance at ambient temperature), load eccentricity, column length

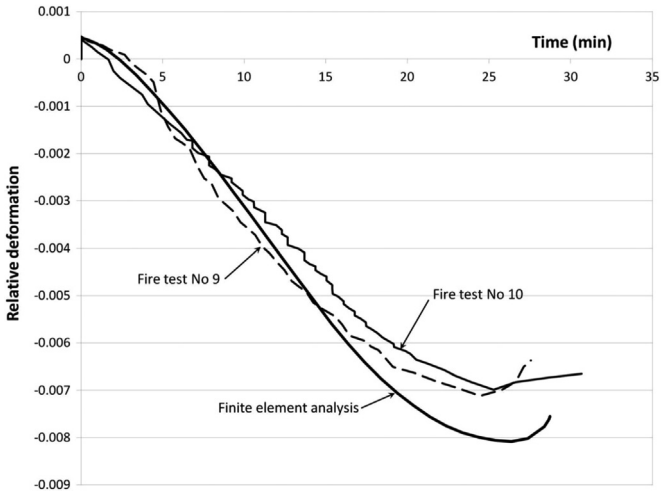

Fig. 9. Comparison of relative deformation-time relationships between experimental and simulation results for the unprotected columns.

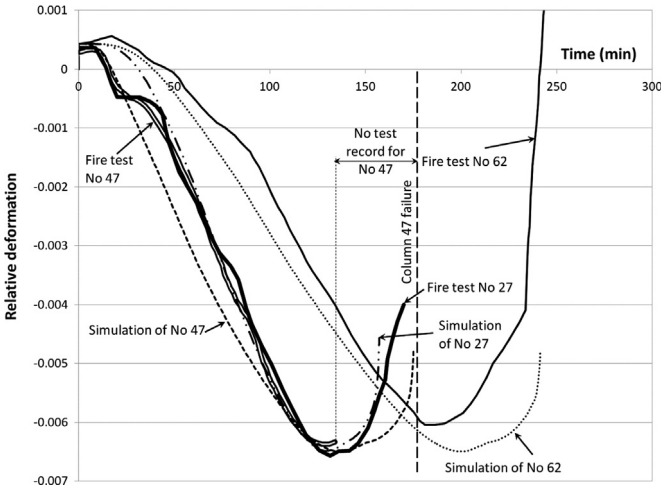

Fig. 10. Comparison of column relative displacement–time relationships between experimental [19] and simulated results for protected columns Nos. 27, 47 and 62.

(slenderness), cross-section imperfection, column length imperfection, boundary condition and level of axial restraint to the column. For the parametric analysis, the simulation model of columns 9 and 10 was used. The parametric study included an additional case in which the boundary condition was changed to simply supported (free rotations) at both ends.

For simulation of columns with axial restraint, a linear elastic axial spring was attached at the column top [30,31]. The spring stiffness k_s is related to the column axial stiffness by a restraint factor α defined below:

$$a=\frac{k_s}{\frac{EA}{L}} \quad (1)$$

where E is the Young's modulus of cast iron, A is the cross section area of the column and L is the length of the column. To assess the range of realistic restraint stiffness, the six storey building described in [32] was used because it had similar columns. The restraint factor was calculated to be about 0.10. In this parametric study, the restraint factor ranges from 0.004 to 0.14.

The standard fire temperature–time curve [33] was used in all simulations.

Table 4 lists the detailed values of the parameters examined.

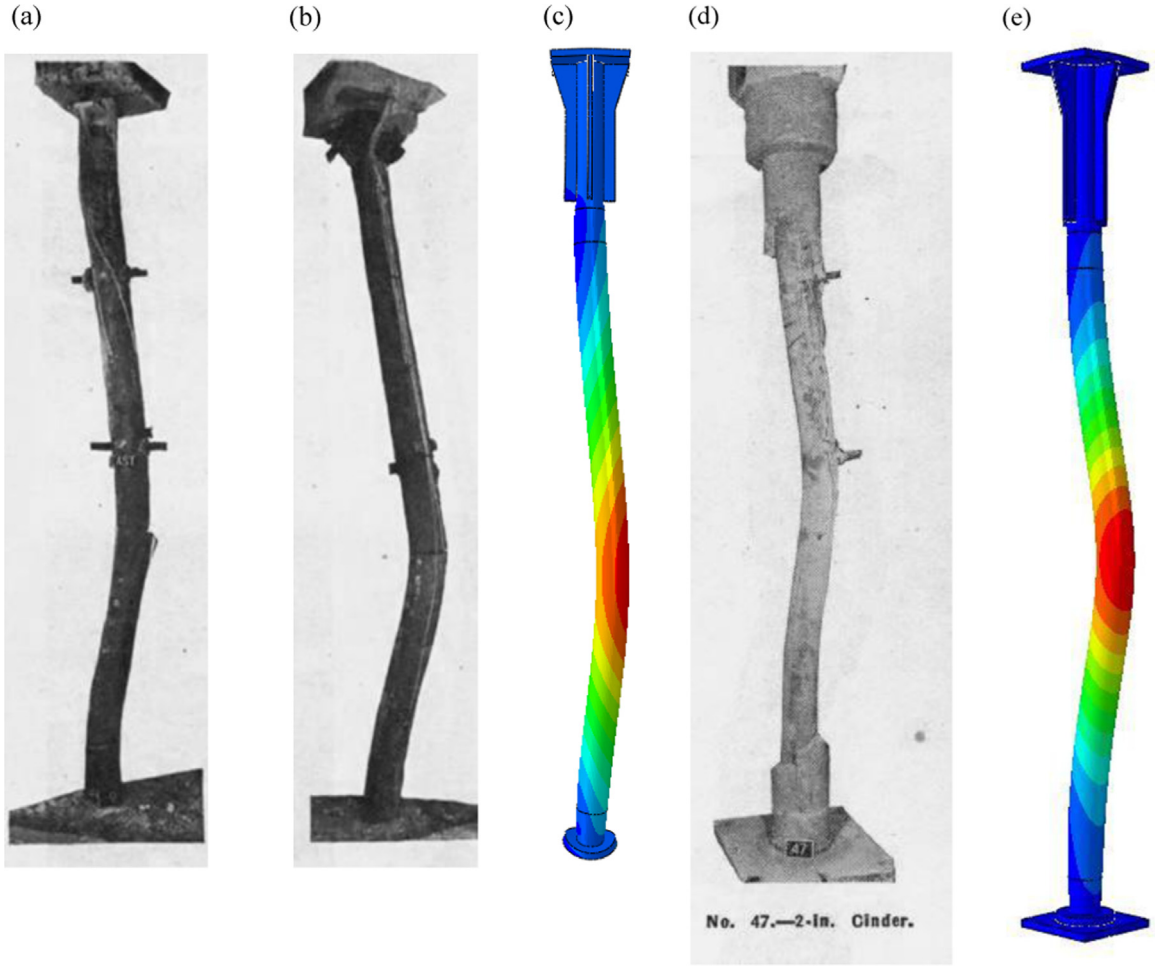

Fig. 11. Comparison for failure modes between fire tests and simulation for unprotected columns, (a) Column 9, test [19], (b) Column 10, test [19], and (c) Columns 9 and 10, simulation, (d) Column 47, test [19] and (e) Column 47, simulation.

Table 3
Comparison of key column behaviour quantities between fire test and numerical results.

Fire test no.	Source	Time of maximum displacement (min)	Fire resistance (min)	Average column temperature at failure (°C)
9	Fire test	24	27	694
	Simulation	25	28	710
10	Fire test	25	31	745
	Simulation	25	28	710
10a	Fire test	17	34	718
	Simulation	20	30	695
27	Fire test	135	178	735
	Simulation	141	170	689
47	Fire test	130	168	710
	Simulation	130	174	715
62	Fire test	175	250	760
	Simulation	175	225	730

4.1. Effects of changing load ratio

Table 5 presents the numerical simulation results.

The design for cast iron structures at the time of construction was very conservative due to the brittle nature of the material and many uncertainties in material properties and construction methods. The safety factor was as high as 5.0. This safety factor combines both the material and load partial safety factors. In contrast, for modern steel structures, the combined safety factor is about 1.5. Taking into consideration the reduced load during fire, the load ratio for modern steel structures is about 0.5. This corresponds to a load ratio of about 0.15 ($=0.5^{*}1.5/5$) for cast iron structures. When historical cast iron structures are refurbished for modern use, it is possible for the excessive margin of safety to be reduced due to better understanding of the material and the structure response. Therefore, it is expected that the load ratio can become considerably higher. To allow for this, the applied load varied from 10% to 200% of the applied load of 425 kN (equivalent to the historic design load) in the parametric study.

Because of the high safety factor, the load utilization factor (ratio of design load to ultimate load carrying capacity) is generally low for cast iron structures, therefore, unprotected cast iron columns can achieve much higher fire resistance time than conventional steel columns. The simulation results indicate that cast iron columns can achieve at least 30 min of standard fire resistance if the applied load is at the historic level of design load (for hinged columns at least 20 min). At very low loads (about 20% of the historic ambient design load), the fire resistance rating approaches 60 min. Even at very high loads (approaching 200% of the historic ambient design load), fixed ends cast iron columns can still achieve 20 min of fire resistance. A further reason is the lower rate of temperature increase in cast iron columns owing to their thicker sections.

4.2. Effects of load eccentricity

Table 6 shows the effects of load eccentricity. The positive eccentricities give higher compressive stress on the thicker part of

Table 4
Summary of input values of parameters examined.

Analysis group no.	Column length (m)	Cross section imperfection, Fig. 3 Diff. max. THK (a) and nominal THK ((D-b)/2) (mm)	Member imperfectionΔ (mm)	Applied load (kN)	Load eccentricity % of cross section width	Relative retrained factor α	Effect of parameter examined
1	Fixed ends 1.88–5.64 50–150% of 3.76 m, increment 10% Hinged ends 2.88–6.64 m Increment 50–150% of 3.76 m	6.35	3.18[a]	425	–	–	Length (slenderness)
2	Fixed ends 3.76	2–14 increment 2	3.18	425	–	–	Cross section imperfection
	Hinged ends 4.76						
3	Fixed ends 3.76	6.35	0–7.95 increment 0.795	425	–	–	Member imperfection
			Fixed ends 3.76 (L/1000) 5.01 (L/750)				
	Hinged ends 4.76		Hinged ends 4.76 (L/1000) 6.35 (L/750)				
4	Fixed ends 3.76	6.35	3.18	85–850 Increment 85	–	–	Load factor
	Hinged ends 4.76						
5	Hinged ends 4.76	6.35	3.18	425 1.5*425	0–80 Increment 10	–	Load eccentricity
6	Fixed ends 3.76	6.35	3.18	425	–	0.004–0.14 Increment 0.008	Axial restraint

[a] Based on measurement of [19].

the section and lower compression stress on the thinner part of the section. In general, the column failure temperature decreases as the eccentricity in either direction increases and is sensitive to the amount of eccentricity. When the applied column load is at the level according to historical design guidance (425 kN for the simulated column), and when the eccentricity exceeds 0.2 D, the column failure temperatures are more than 50 °C lower than those without eccentricity. Increasing the applied load accelerates this effect.

Later in Fig. 12, the simulation results will be used to assess calculation results using the Eurocode design method for steel columns. For this assessment, the simulation results for eccentricity of 0.2 D and less will be included. For higher values of cross-section eccentricity, it is no longer appropriate to treat the column as under compression only and explicit consideration of column eccentricity should be taken.

4.3. Effects of cross section imperfection

Due to imprecision in manufacturing cast iron sections, cast iron columns usually have some cross section imperfection where the thickness of the section varies. This can have a number of effects. (1) the thinner part of the cross section develops higher temperature than the thicker part. This causes thermal gradient in the cross section and hence additional bending moment in the column when the applied compressive load acts on the thermal bowing induced by the thermal gradient. As the length of the column increases, the additional bending moment also increases. (2) The non-uniform temperature within the cross section causes redistribution of stresses: the thinner part would have lower stress, due to higher temperature, than the thicker part. This would adversely affect the overall stiffness of the cross section because non-uniform distribution of stiffness of the material causes the highly stressed part to lose stiffness earlier.

Combining these two effects, it is expected that cross section imperfection would have more severe effects on more slender columns. The results in Fig. 7 confirm this expectation. For columns with fixed ends which have low slenderness (length 3.76 m, ambient temperature slenderness $\bar{\lambda}$=0.477), the failure of the columns is controlled by the cross section materials reaching their strength. This is compatible with the findings of [4] where the authors indicate that cross section eccentricity reduces cast iron column resistance by no more than 3% at ambient temperature. For columns with hinged ends, because the column slenderness is high (length 4.76 m, $\bar{\lambda}$=1.2), cross section imperfection becomes an important parameter and can have severe detrimental effects on column fire resistance and failure temperature (Table 7).

4.4. Effects of column imperfection

As with modern steel columns, cast iron columns also have column imperfection (initial deflection). In [4], the magnitude of cast iron column imperfection has been assessed, giving a mean value of L/1500 and a maximum value of L/750. These are comparable to a value of L/1000 [4] which is typically considered for modern steel columns. Table 8 presents the simulation results. Column imperfection has the same effect as load eccentricity: introducing bending moment in the column. Because the column initial imperfection is small, it has very small influence on column fire resistance.

4.5. Effects of axial restraint

Table 9 summarizes the simulation results of the effect of axial restraint on fire resistance. It can be seen that axial restraint to cast iron column can result in significant reductions in column fire

Table 5
Effects of load ratio on fire resistance and failure temperature of cast iron column.

Applied load (kN)	% of ambient temperature design load	% of ambient temperature section capacity (fy*A)	Fixed ends column		Hinged ends column	
			Fire resistance (min)	Failure temperature (°C)	Fire resistance (min)	Failure temperature (°C)
85	20	9.30	74.52	967	40.04	762
170	40	18.5	47.20	844	32.0	715
255	60	27.9	41.28	777	24.52	644
340	80	37.2	33.5	735	21.06	580
425	100	46.5	28.72	706	19.9	555
510	120	55.8	26.72	681	18.6	525
595	140	65.1	25.18	658	16.93	486
680	160	74.4	23.92	637	15.4	450
765	180	87.3	22.87	618	14.38	418
850	200	93.0	21.93	600	12.43	356

resistance and failure temperature. This is caused by the increased compression in the column due to restrained thermal expansion. For example, the fire resistance period without axial restraint is nearly 30 min (failure temperature=706 °C) when the column is axially unrestrained, but they decrease to 20.5 min (571 °C) respectively when the axial restraint factor is $\alpha=0.14$. It is important that the axial restraint is reliably estimated and the increased compression force is accurately calculated.

The increased compressive force in axially restrained column can be calculated using the following relationship [34]:

$$\Delta P = \frac{K_s K_c}{K_s + K_C}(\Delta\varepsilon_{th} - \Delta\varepsilon_{mec})L \quad (2)$$

where K_s and K_c are the stiffness of the axial restraint and the stiffness of the column at the relevant elevated temperature, $\Delta\varepsilon_{th}$ is the free thermal strain of the column as a result of temperature increase, $\Delta\varepsilon_{mec}$ is the column mechanical strain increase due to column reduction in the material stiffness when the temperature is increased. $\Delta\varepsilon_{mec}$ is generally very small for the strain levels of cast iron columns and can be ignored. $\Delta\varepsilon_{th}$ is given by the thermal elongation relationship in EN 1993-1-2 [23]. Table 9 confirms that the analytical Eq. (2) gives accurate calculations of the increased column axial force. The analytical equation tends to slightly overestimate the additional compressive force in the column. This happens because in the simulation model, the cross section eccentricity was included; this caused the column to deform laterally thereby reducing the axial expansion. This second order effect cannot be included in the analytical model, however, this places the analytical results slightly on the safe side.

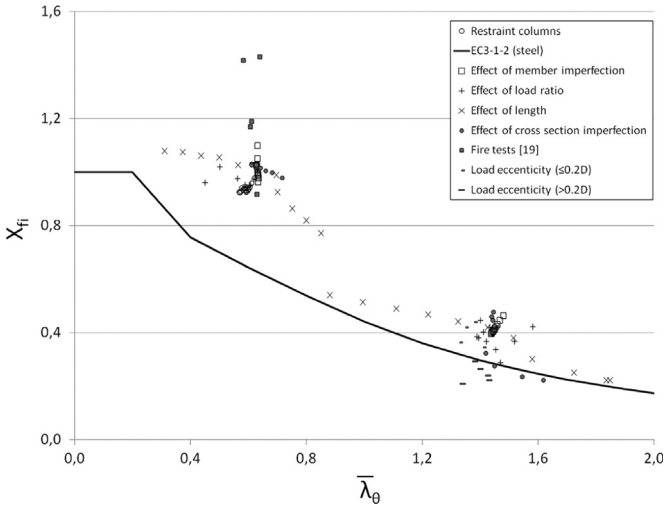

Fig. 12. Reduction factor vs elevated temperature slenderness for the tested columns [19] and the simulation results.

The results in Table 9 indicate that at realistic axial restraint levels (about 0.10 in Section 4), the total compression in the column may double the initial load in the column. This has resulted in a reduction of column failure temperature by more than 100 °C (i.e. 706–594 °C).

Table 6
Effect of load eccentricity.

Column with hinged ends applied load 425 kN			Column with hinged ends applied load 1.5 *425 kN=637.5 kN		
Load eccentricity (D)	Fire resistance (min)	Failure temperature (°C)	Load eccentricity (D)	Fire resistance (min)	Failure temperature (°C)
+0.7	11.44	325.3			
+0.6	14.67	422.13	+0.6	–	20
+0.5	16.03	459.78	+0.5	2.64	64.3
+0.4	17.05	486.89	+0.4	6.83	180.95
+0.3	17.98	510.14	+0.3	9.86	275.86
+0.2	18.87	531.71	+0.2	12.75	365.3
+0.1	19.83	553.44	+0.1	15.51	445.66
0	21.04	579.43	0	17.8	505.8
−0.1	20.58	569.78	−0.1	17.24	491.64
−0.2	19.34	542.48	−0.2	15.09	434.04
−0.3	17.84	506.75	−0.3	–	20
−0.4	16.44	470.77			
−0.5	14.91	428.85			
−0.6	13.10	376.05			
−0.7	10.53	292.10			

Table 7
Effect of cross section imperfection to fire resistance and critical temperature.

Cross section imperfection ratio (imperfection/cross section diameter (D))	Fixed ends column Fire resistance (min)	Fixed ends column Failure temperature (°C)	Hinged ends column Fire resistance (min)	Hinged ends column Failure temperature (°C)
0.01125	29.18	711	21.7	595
0.0225	29.13	710	21.35	590
0.03375	28.99	709	21.165	582
0.045	28.90	708	18	528
0.05624	28.68	706	16.3	484
0.0675	28.43	705	14.61	425
0.07874	28.21	701	13.79	389

Table 8
Effects of column imperfection on column fire resistance and failure temperature.

Column with fixed ends			Column with hinged ends		
Δ/D ratio (10^{-3}) (−)	Fire resistance (min)	Failure temperature (°C)	Δ/D ratio (10^{-3}) (−)	Fire resistance (min)	Failure temperature (°C)
0	29.16	710	0	22.5	596
4.471	29.02	709	4.471	21.87	590
8.943	28.91	708	8.943	21.24	584
13.414	28.8	707	13.414	21.15	581.5
17.885	28.7	706	17.885	21.06	579
22.357	28.61	705	22.357	20.965	577.5
26.828	28.52	704	26.828	20.87	576
31.299	28.43	703	31.299	20.785	574.5
35.771	28.35	702	35.771	20.7	573
40.242	28.26	701	40.242	20.615	571
44.713	28.10	699	44.713	20.53	569
21.147 (L/1000)	28.64	705	26.772 (L/1000)	20.87	576
28.178 (L/750)	28.49	703	35.658 (L/750)	20.7	572

5. Assessment of applicability of EN 1993-1-2 to cast iron columns

For steel columns, according to EN 1993-1-2 [23], the design compression resistance $N_{b,fi,t,Rd}$ at time t of a compression member with a uniform temperature θ is:

$$N_{b,Rd,\theta}=\frac{\chi_{fi}*A*k_{y,\theta}*f_y}{\gamma_{M,fi}} \quad (3)$$

where χ_{fi} is the reduction factor for flexural buckling in the fire design situation, $k_{y,\theta}$ is the reduction factor of the yield strength of steel, f_y is the yield strength of steel, A is the area of the column's cross section and $\gamma_{M,fi}$ is the material safety factor for fire design. In this assessment, the material safety factor $\gamma_{M,fi}$ is equal to 1.0.

The strength reduction factor χ_{fi} is calculated using the following equation:

$$\chi_{fi}=\frac{1}{\varphi_\theta+\sqrt{\varphi_\theta^2-\bar{\lambda}_\theta^2}} \quad (4)$$

with

$$\varphi_\theta=\frac{1}{2}*[1+\alpha*\bar{\lambda}_\theta+\bar{\lambda}_\theta^2] \quad (5)$$

and

Table 9
Effects of axial restraint

Restraint factor α	Fire resistance (min)/Failure temperature (°C)	Simulation result of column axial force (kN)	Analytical result of column axial force (kN)
0.000	28.7/706	425	425
0.004	28.1/697	452.32	451.35
0.012	26.9/683	503.22	501.5
0.020	26.0/670	549.74	548.53
0.028	25.2/658	592.26	592.82
0.036	24.6/648	631.04	635.12
0.044	24.0/639	665.68	675.51
0.052	23.6/631	696.25	714.3
0.060	23.2/624	723.96	751.8
0.068	22.9/617	756.51	787.56
0.076	22.5/611	785.85	822.43
0.084	22.2/605	817.01	855.81
0.092	21.9/599	842.26	887.72
0.100	21.6/594	869.93	919.23
0.108	21.4/589	893.93	949.49
0.116	21.1/584	918.86	978.53
0.124	20.9/579	941.59	1006.38
0.132	20.7/574	966.23	1033.1
0.140	20.5/571	983.12	1061.34

$$a=0.65*\sqrt{235/f_y} \quad (6)$$

The column slenderness $\bar{\lambda}_\theta$ at elevated temperature θ is calculated by:

$$\bar{\lambda}_\theta=\bar{\lambda}*\sqrt{k_{y,\theta}/k_{E,\theta}} \quad (7)$$

where $k_{y,\theta}$ and $k_{E,\theta}$ are the reduction factors for yield strength and Young's modulus for steel at temperature θ and $\bar{\lambda}$ is the ambient temperature slenderness, defined by EN 1993-1-1 [35].

For application to cast iron columns, the following modifications are made:

- The yield strength of steel is replaced by the 0.2% proof stress and the temperature – dependent reduction factors are the same as those for the yield strength of steel, according to [25].
- The ambient temperature modulus of elasticity for cast iron in compression is 103.95 GPa (used in the numerical simulations, and according to [19]).
- The effective length factor is 1.0 for hinged ends and 0.5 for fixed ends.
- The column is assumed to have uniform temperature distribution in the cross-section and the average cross-section temperature is used.
- For axially restrained columns, the applied load is the maximum force in the column due to restrained thermal expansion.

Fig. 12 compares all the simulation results with calculation results using the Eurocode 3 Part 1–2 method (described above) for steel columns. In general, the analytical method gives conservative (safe) results. The results in Fig. 12 also show that if the column load eccentricity does not exceed 0.2 D, using the EN 1993-1-2 design equation gives reasonably accurate and safe estimation of the limiting temperatures of cast iron column even if the effects of load eccentricity are not included. However, if the load eccentricity exceeds 0.2 D, it is no longer safe to assume the column to be under compression only.

For stocky columns, the margin of safety is quite high. In fact, because the cross-section average temperature is used and the thicker part of the cross-section has lower temperatures, the column failure load may be even higher than the calculated plastic resistance of the cross-section with average uniform temperature.

Nevertheless, it is considered not necessary to search for a

more refined, and hence more accurate, method to calculate cast iron column resistance at elevated temperatures. Cast iron structures are no longer being constructed and there is not a very strong economic drive to reduce construction cost. Therefore, as long as the assessment method is safe and reasonably accurate, it is considered acceptable.

6. Conclusions

The paper has presented the results of a numerical investigation of the behaviour of cast iron columns in fire. The finite element models, using ABAQUS, for both heat transfer modeling and structural modeling, were validated against fire tests [19].

The validated numerical models were used to investigate how different design parameters affect the limiting temperature of cast iron column and load carrying capacity at elevated temperature. The parameters considered include: column slenderness, load factor, load eccentricity, imperfections of column and cross section and axial restraint. The parametric study results were used to assess applicability of using the current fire resistant design method for steel columns in EN 1993-1-2 to cast iron columns. From this study, the main conclusions are as follows:

- Loading eccentricity should be no more than 0.2 D. Columns with higher eccentricities should be explicitly treated as members with combined axial compression and bending.
- The effects of cross-section and column imperfections are minor and can be adequately represented by using an appropriate column buckling curve.
- Axial restraint to cast iron columns can generate significant additional compression forces and decrease the column limiting temperatures. This should be considered in practical assessment.
- The Eurocode 3 Part 1–2 analytical method for steel columns can be safely used for cast-iron columns.

Acknowledgements

The authors would like to thank Dr. Sara E. Wermiel of M.I.T. for providing the cast iron fire test report [19].

References

[1] M. Bussell, Use of iron and steel in buildings, in structures and construction, in: M. Forsyth (Ed.), Historic Building Conservation, Blackwell Publishing Ltd, Oxford, UK, http://dx.doi.org/10.1002/9780470691816.ch10.
[2] Institution of Structural Engineers, Appraisal of existing structures, 2nd edition, The Institution of Structural Engineers, London, UK, 1996.
[3] D. Friedman, Cast-iron-column strength in renovation design, J. Perform. Constr. Facil. 9 (3) (1995) 220–230.
[4] J. Rondal, K.J.R. Rasmussen, On the strength of cast iron columns, J. Constr. Steel Res. 60 (2003) 1257–1270.
[5] I. Brooks, A. Browne, D.A. Gration, A. McNulty, Refurbishment of St Pancras – justification of cast iron columns, Struct. Eng. 3 (2008) 28–39.
[6] T. Swailes, E.A. Fernandez de Retana, The strength of cast iron columns and the research work of Eaton Hodgkinson (1789-1861), Struct. Eng. 82 (2) (2004) 18–23.
[7] C. Paulson, R.H.R. Tide, D.F. Meinheit, Modern techniques for determining the capacity of cast iron columns, in: S.J. Kelly (Ed.), Standards for Preservation and Rehabilitation, ASTM STP 1258, American Society for Testing and Materials, Texas, USA, 1996, pp. 186–200.
[8] G.G. Nieuwmeijer, Fire resistance of historic iron structures in multistory buildings, Trans. Built Environ. 55 (2001) 39–48.
[9] A. Baxter, New concordia wharf, fire engineering aspects, Archit. J. 180 (27) (1984) 58.
[10] A. Porter, The behavior of structural cast iron in fire, Engl. Herit. Res. Trans. Vol. 1 (1998) 11–20.
[11] I.L. Twilt, Fire resistance of cast iron structures in historic buildings, Urban Herit. Build. Maint. Iron Steel Neth. (1999) 99–106.
[12] D. Dibb-Fuller, R. Fewtrell, R. Swift, Windsor Castle: fire behaviour and restoration aspects of historic ironwork, Struct. Eng. 76 (19) (1998) 367–372.
[13] F.L. Brannigan, Cast iron and steel, Fire Eng. 159 (2006) 126.
[14] Fire resistance, BCIRA Broadsheet, 283/1, UK, 1988.
[15] Cast iron in building structures, revived interest in a proven case, BCIRA Report X 181, UK, 1984.
[16] Experiences with cast-iron columns in two English spinning mill fires, Engineering News, January 1, 1903, p. 21.
[17] How structural cast-iron behaves in a fire, Foundry Trade Journal, May 25, 1967, p 613.
[18] J.R. Barnfield, A.M. Porter, Historic buildings and fire: fire performance of cast-iron structural elements, Struct. Eng. 62A (12) (1984) 373–380.
[19] Associated Factory Mutual Fire Insurance Companies, The National board of Fire Underwriters and the Bureau of Standards, Department of Commerce (1917–1919): Fire Tests of Building Columns, Underwriters' Laboratories, Chicago, Illinois, USA.
[20] S.A. Reed, Work of the committee of fire-proofing tests, Journal. Frankl. Inst. State Pa. CXLII (5) (1896) 321–335.
[21] I. Wouters, M. Mollaert, Evaluation of the fire resistance of 19th century iron framed buildings, Fire Technol. 38 (2002) 383–390.
[22] F. Wald, M. Dagefa, Fire resistance of cast iron columns, J. Struct. Fire Eng. 4 (2) (2013) 95–102.
[23] European Committee for Standardization. Eurocode 3-Design of steel structures – Part 1-2: General rules – Structural fire design. Brussels: The Committee, 2005.
[24] C. Maraveas, Y.C. Wang, T. Swailes, Thermal and mechanical properties of 19th century fireproof flooring systems at elevated temperatures, Constr. Build. Mater. 48 (2013) 248–264.
[25] C. Maraveas, Y.C. Wang, T. Swailes, G. Sotiriadis, An Experimental Investigation of Mechanical Properties of Structural Cast Iron at Elevated Temperatures and after Cooling Down, Fire Saf. J. 71 (2015) 340–352.
[26] The London County Council (General Powers) Act 1909: 9 Ed VII Cap CXXX, HMSO, 1909.
[27] C. Maraveas, Y.C. Wang, T. Swailes, Fire resistance of 19th century fireproof flooring systems: a sensitivity analysis, Constr. Build. Mater. 55 (2014) 69–81.
[28] European Committee for Standardization. Eurocode 2-Design of concrete structures – Part 1-2: General rules – Structural fire design. Brussels: The Committee, 2004.
[29] European Committee for Standardization. Eurocode 1 – Actions on structures – Part 1-2: General rules – Actions on structures exposed to fire. Brussels: The Committee, 2002.
[30] F.A. Ali, I.W. Simms, D.J. O'Connor, Behaviour of axially restrained steel columns during fire, Fire Safety Science, vol. 5, pp. 1105–1116. doi:10.3801/IAFSS.FSS.5-1105.
[31] P. Shepherd, The Performance in Fire of Restrained Columns in Steel-Framed Construction (Ph.D. thesis), University of Sheffield, Sheffield, UK, 1999.
[32] M.N. Bussell, M.J. Robinson, Investigation, appraisal, and reuse, of a cast-iron structural frame, Struct. Eng. 76 (3) (1998) 37–42.
[33] Fire resistance tests-elements of building construction—Part 1: General requirements. International Standard ISO 834-1, 1999.
[34] Y.C. Wang, Postbuckling behaviour of axially restrained and axially loaded steel columns under fire conditions, J. Struct. Eng. 130 (3) (2004) 371–380.
[35] European Committee for Standardization. Eurocode 3-Design of steel structures – Part 1-1: General rules and rules for buildings. Brussels: The Committee, 2005.